The NASA Optical Communication and Sensor Demonstration Program: An Update

Siegfried W. Janson and Richard P. Welle
The Aerospace Corporation
Mail Stop M2/241, P.O. Box 92957, Los Angeles, CA 90009-2957; 310.379.7060
siegfried.w.janson@aero.org

ABSTRACT

The Optical Communication and Sensor Demonstration Program was one of three projects selected by the NASA Small Spacecraft Technology Program in 2012. This effort will demonstrate a 5 to 50 Mbps optical downlink in a 1.5U CubeSat based on a 10-W modulated fiber laser with a 0.35^{o} full width half-maximum angular beamwidth. To fully utilize the laser, the spacecraft requires equivalent or better pointing accuracy. We've developed miniaturized sun, Earth Nadir, and Earth-horizon sensors, plus a cm-scale star tracker, to provide the required attitude references for our attitude control system.

The secondary goal is to demonstrate proximity operations using two identical spacecraft. In the spring of 2015, two 1.5U AeroCube-OCSD CubeSats will be ejected from the same P-POD and brought within 200-meters of each other using on-board GPS measurements for position and velocity determination, variable drag for cooperative orbit rephasing, and a steam thruster for proximity maneuvering. Each satellite has deployed wings that allow varying the ballistic coefficient by at least a factor of 4 by changing spacecraft orientation with respect to the flight direction. High-fidelity orbit ephemerides will be generated on the ground using multiple GPS measurements per orbit, and relative range will be measured on-orbit using a laser rangefinder.

1.0 NASA'S SMALL SPACECRAFT EFFORTS

The Optical Communication and Sensor Demonstration is a two-CubeSat flight test funded by NASA's Small Spacecraft Technology Program (SSTP) under the Space Technology Mission Directorate. Other SSTP efforts include ISARA, CPOD, PhoneSat and the eight-CubeSat Edison Demonstration of SmallSat Networks (EDSN).[1]

2.0 WHY LASER COMMUNICATIONS?

Advances in micro/nanoelectronics have enabled unprecedented data collection and storage capabilities in spacecraft of all sizes. A current generation 15-megapixel color imager operating at 30 Hz can generate over 10 gigabits/s of raw data. Even with low-loss video compression, data rates can easily exceed 200 megabits/s. Recording this compressed video over an entire orbit would require about 132 GBytes; slightly more than the 128 GByte storage capacity of a micro SD flash memory card. A terabyte of data can be readily stored in a CubeSat, and with a little more effort, over 10 Terabytes is possible.

Sending this amount of data from a power and antenna-gain limited small satellite to the ground is a challenge. A good S-band CubeSat downlink can handle a data rate of several megabits/s. Downloading a terabyte using a single ground station at a rate of 5 megabits/s (Mbps) with an average of four 10-minute passes per day (very optimistic) would take almost 2 years. Storing terabytes of information is easy; sending it to the ground is hard. Either an order-of-magnitude or more increase in the number of ground stations, or an equivalent increase in downlink data rates, is required to enable more reasonable data download times.

Laser communications offer gigabit/s data rates; a several order-of-magnitude increase in rate compared to radio frequency (RF) communications. NASA's Lunar Laser Communication Demonstration (LLCD), an experiment on the Lunar Atmosphere and Dust Environment Explorer (LADEE), sent data from lunar orbit to the Earth in late 2013 at a record-breaking rate of 622 Mbps. This was six times faster than previous RF communications from the moon, using a transmitter with half the weight and one quarter the input power of an equivalent RF system. Note that communications from the moon, with a link length of about 400,000 km,

is many orders-of-magnitude harder than from low Earth orbit (LEO), with a link length of about 1000 km.

Optical satellite-to-ground data rates in excess of 5-Gbps have already been demonstrated using LEO spacecraft. Members of The Aerospace Corporation, in collaboration with Tesat-Spacecom, previously demonstrated 5.625-Gbps bidirectional laser communications between a 6.5-cm-diameter ground station at the European Space Agency Optical Ground Station in Izana, Tenerife, and a 12.5-cm-diameter terminal mounted on the Near Field Infrared Experiment (NFIRE) satellite in low Earth orbit (LEO).[2] The spacecraft terminal had a mass of 35-kg, a power consumption of 120 W, dimensions of 0.5 x 0.5 x 0.6 m, and transmitted 0.7 W at 1064 nm wavelength.[3] This high-performance system with a ~50-microradian angular beam width and gimbaled pointing system would obviously not fit in a CubeSat.

Eliminating the optical gimbal and increasing the angular beam width to several milliradians to allow spacecraft body-pointing of the laser, enables a significantly smaller, lighter optical terminal. This approach takes advantage of the exceptionally low moments-of-inertia of CubeSats, and their ability to perform rapid slew maneuvers. Our CubeSats can typically rotate about a single axis at rates of 10^o to 20^o per second.

Figure 1 shows the angular rate and range for a spacecraft in a 600 km altitude orbit with a vertical pass over an optical ground station. Required rotation rates are less than 0.8^o/s, and overhead passes at lower maximum elevation will have even lower rotation rate requirements. For OCSD, we have chosen a maximum link length of 900 km. At 600 km altitude, this yields a minimum elevation angle of 30^o, and a maximum laser communications period of 180 s.

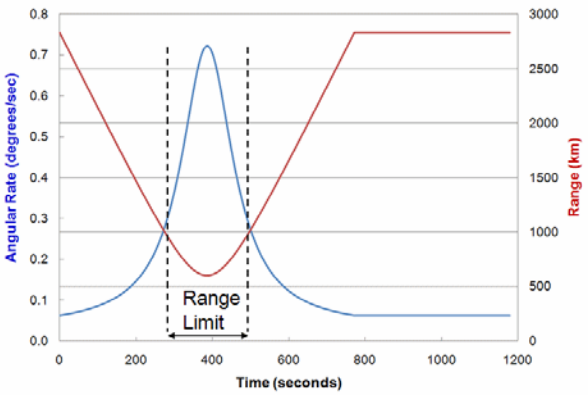

Figure 1. Angular rates and range as a function of time for a spacecraft passing over a ground station with a maximum elevation of 90^o.

3.0 THE OCSD FLIGHT DEMONSTRATION

The OCSD flight hardware consists of two, 1.5U CubeSats that will be ejected from a single CubeSat deployer in the spring of 2015. Each spacecraft can perform the primary optical communications mission independently, but two spacecraft are required to perform a secondary mission of demonstrating proximity operations.

Overall, the OCSD effort will demonstrate a number of useful small satellite technologies:

1. Optical communications from a CubeSat to a 30-cm-diameter ground station from low Earth orbit at a rate of 5 to 50 Mbps,
2. Tracking of a nearby, cooperative spacecraft using a commercial, off-the-shelf (COTS) laser rangefinder,
3. Attitude determination using a sub-cubic inch star tracker and a number of COTS optical thermometers,
4. Orbit rephasing using variable aerodynamic drag, and
5. Orbit control using a safe, non-toxic, easy to flight-qualify, steam thruster.

Unlike our previous paper, this paper will focus on all five technologies.[4]

4.0 THE SPACECRAFT

Figure 2 shows a rendering of an AeroCube-OCSD spacecraft. Each 1.5U CubeSat has two deployable wings to provide a wide range (5 to 1) of ballistic coefficient to enable orbit control through variable aerodynamic drag. Variable drag will be used to control inter-spacecraft range when ranges exceed 1 km.

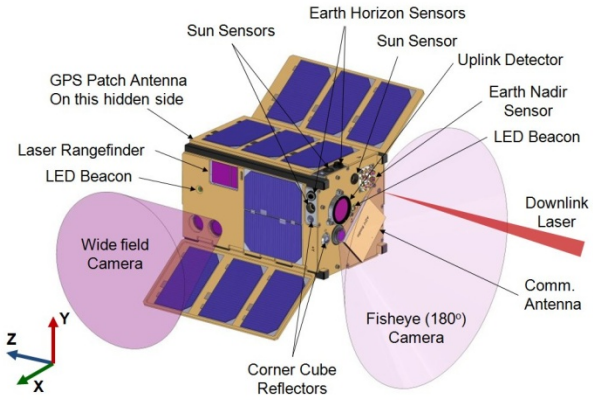

Figure 2. Rendering of the OCSD CubeSat.

The wing surfaces and two of the rectangular side panels have three, ~1-W, triple-junction solar cells, while each of the remaining two rectangular side panels have a single, 2-W triple-junction cell. Maximum solar input power is 9.5 W, and typical orbit-average power in the expected orbit is 4.5 W. Two COTS 18650 size "high energy" lithium ion batteries with a total capacity of 14 W-hr provide spacecraft power during eclipse, and two COTS "high current" 18650 size lithium ion batteries provide over 50 W to the laser transmitter during optical downloads. These "high current" batteries are typically used to power hand-held portable drills and other power tools.

4.1 Coarse Attitude Sensors

Since both spacecraft can and will fly with a wide range of orientations to support optical downlink and proximity operations, we incorporated six 2-axis sun sensors, four Earth horizon sensors, a two-axis Earth nadir sensor, and two sets of 3-axis magnetometers as basic attitude sensors. This combination of sensors allows continuous attitude determination with ~1° accuracy even with multiple attitude sensor failures.

Our sun and Earth nadir sensors, described in previous work, have successfully flown on three different spacecraft missions.[5,6] Once calibrated, our sun sensors have a 0.32° root mean square (rms) error, over a 35° field-of-view, in two axes. Based on flight data from multiple missions, our Earth nadir sensor has 1° accuracy in two axes. Errors typically result from using COTS optical temperature sensors that see thermal radiation from 5 to 14 microns in wavelength. Parts of this band can see all the way to the ground while other parts only see high altitude clouds that are typically cold.

Our chip-scale magnetometers also have roughly 1° accuracy in two axes when instantaneous position is known and the local field is interpolated from an up-to-date magnetic field table. Magnetic field bias errors from magnetized batteries, other ferromagnetic parts, and permanent magnets in reaction wheels and other components contribute to this error.

Each spacecraft has four COTS Melexis MLX90620 infrared array sensors as an attitude-determination experiment to locate the Earth's warm limb against cold space. These sensors have a 4 x 16 array of thermopile temperature sensors that can optically read temperature with a 0.25 K (rms) temperature difference from -50 °C to 300 °C at a 4 Hz rate.[7] Each pixel has a 3.75° x 3.75° FOV, potentially enabling nadir determination accuracy of ~0.3° when all four sensors can see the Earth's limb. These sensors provide a backup to the legacy Earth nadir sensor and should be less affected by cold, high-altitude clouds.

4.2 Fine Attitude Sensors

Precision pointing for laser communications using our 0.35° FWHM downlink beam width requires a 0.175° spacecraft-to-ground-station pointing accuracy that is much tighter than the ~1° pointing accuracy provided by our legacy attitude sensors. We added closed-loop control for tracking the laser ground station by integrating a modulated, 10-W, 1550-nm, laser uplink at the ground station, co-aligned with the telescope receiver, and a lensed photodiode receiver on the satellite to provide better than 0.1° pointing at the ground station during an overhead pass. The uplink receiver consists of narrow-band-pass filter followed by an 18-mm diameter lens that focuses incoming light onto a 3-mm diameter InGaAs quad photodiode. Individual currents from each of the four diodes are used to generate error signals for each of two axes, while the summed output provides data. The optical uplink data rate is less than 10 kilobits/s.

Closed-loop optical feedback is also used to aim each CubeSat laser rangefinder at the other CubeSat with better than 0.1° accuracy. The initial crude pointing direction for each spacecraft is pre-calculated on the ground as a function of time using high-precision orbital elements based on multiple, recent (within 24-hours), GPS fixes over one or more orbits. Our flight-proven GPS receivers have a single point positional accuracy of ~20 meters, resulting in instantaneous in-track and cross-track positional of about 10 meters when using multiple GPS fixes over an orbit, high precision orbit fitting, and uploaded pointing tables. At an inter-satellite range of 200 meters, a 10-meter error for each spacecraft results in a maximum angular pointing error of 5.7°.

Cooperative, closed-loop tracking starts with each spacecraft aiming the +X body vector at the other spacecraft (see Fig. 2), using the uploaded pointing data and the current time. A red, 670-nm-wavelength, LED on the +X face of the intended "target" spacecraft is turned on, and the "chase" spacecraft takes a picture using the color wide field camera on it's +X face. The 10-megapixel (10MP) color wide field camera has a 38° diagonal field of view, co-aligned with the +X surface, and the 0.3-W output LEDs have a 60° full-width half-maximum (FWHM) angular beam width, also co-aligned with the +X surface. For typical conditions and ranges in excess of 200 meters, the +X LED will be within the camera FOV. Two more LEDs, one on the +Z and one on the –Z face, were added for potential "lost in space" conditions that can occur when the

spacecraft are closer than 200 meters, and/or when GPS-derived pointing vectors are "stale". This can occur if the elements are more than a few days old, or when atmospheric densities suddenly change due to a solar event.

An on-board Xilinx Spartan-6 family field-programmable gate array reads an image frame from the color camera, finds the brightest red "dot", and calculates X and Y error angles based on the dot centroid location within the imager array. With a two-pixel centroid location accuracy due to the color filter pattern on the imager, this system provides 0.016^{o} pointing accuracy; well within the 0.09^{o} angular beam width of the laser rangefinder.

Figure 3 shows the calculated visual magnitude for our LED as a function of range, and has been verified using a ground test with an 800-meter range. Our Aptina MT9D131 2MP color imager on AeroCube-4 sees stars down to 5.8^{th} magnitude using a 16-mm focal length, f/2 lens. The 10MP Aptina MT9J003 wide field color imager on this spacecraft is one third as sensitive, but will use an f/1.6 lens to increase light collection by 50%. The 10MP wide field camera should see stars down to 5^{th} magnitude using equivalent exposure times. Color and brightness will be used to determine whether a particular bright spot in the camera FOV is a star, planet, or red LED. Overall, an individual LED should be seen by our wide field camera out to 10-km range.

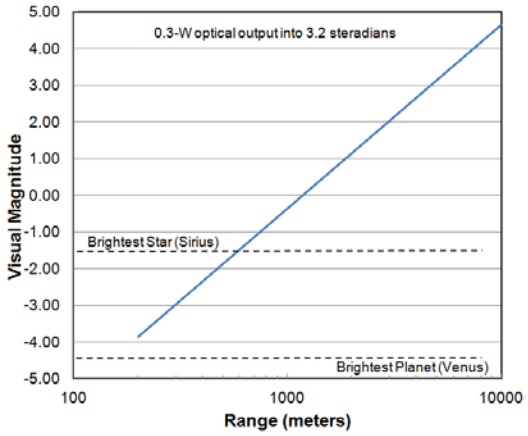

Figure 3. Visual magnitude of a 0.3-W, 60^{o} FWHM beam pattern, red LED as a function of distance when the LED is aimed at the observer.

Dual star trackers on each OCSD CubeSat use an Aptina MT9V022 monochrome WVGA imager with five times the sensitivity of those on AeroCube-4. These imagers are coupled to f/1.2 lenses, compared to f/2.0 for AeroCube-4, resulting in 3 times the light collection capability. A Spartan-6 FPGA reads an image frame, processes the field, and outputs a collection of star locations. These data are further processed by a 16-bit microcontroller using a star catalog to output pointing direction as a set of quaternions. One star tracker points in the +Z direction (typically zenith), while the other is canted by 40^{o} to provide angular diversity in case stray light from the moon, sun, etc. interferes with one tracker. Star fields are imaged about once per second, and quaternion outputs are combined with more rapid rate gyro data to provide continuous attitude information with less than 0.1^{o} error.

For robustness and power control, we have two 3-axis rate gyros on each spacceraft. A Sensonor STIM-210 3-axis rate gyro provides a bias stability of $0.5^{o}/(hour)^{1/2}$, but it has a maximum power consumption of 1.5 W and needs a one hour warmup period.[8] These devices are susceptible to helium exposure that can occur during launch vehicle preparations, so we mount them inside their own hermetically-sealed container. We discovered this issue on AeroCube-4 using the legacy STIM-202.

Another set of rate gyros is in the VectorNav VN-100 inertial measurement unit (IMU), also on each spacecraft.[9] These gyros provide a bias stability $\sim 10^{o}/(hour)^{1/2}$, but the IMU consumes only 0.33 W. This IMU also contains a 3-axis set of accelerometers, a 3-axis set of magnetometers, and a pressure sensor.

4.3 Attitude Actuators

Attitude actuators include a triad of magnetic torque rods and a triad of reaction wheels. Our torque rods have a magnetic moment of 0.2-A-m^2. They provide torques for detumbling and reaction wheel unloading. Our reaction wheels have flight heritage on multiple spacecraft with 1-mN-m-s of total angular momentum. Spacecraft slew rates can be in excess of 5^{o} per second, and pointing control to within 0.1^{o} has been demonstrated on-orbit using a similar spacecraft.

5.0 THE OPTICAL DOWNLINK

Our 1064-nm wavelength optical downlink uses a low power amplitude-modulated diode laser followed by two polarization-maintaining ytterbium-doped fiber amplifier stages. Figure 4 shows a schematic drawing of the laser design. Our initial breadboard design used highly efficient optical pumping at 975 nm, but this proved to be unworkable over the expected 0 to 40^{o} C range in laser system temperature on orbit. The 975-nm absorption feature is narrow, and temperature-stabilized pump lasers capable of maintaining this wavelength stability were too inefficient.

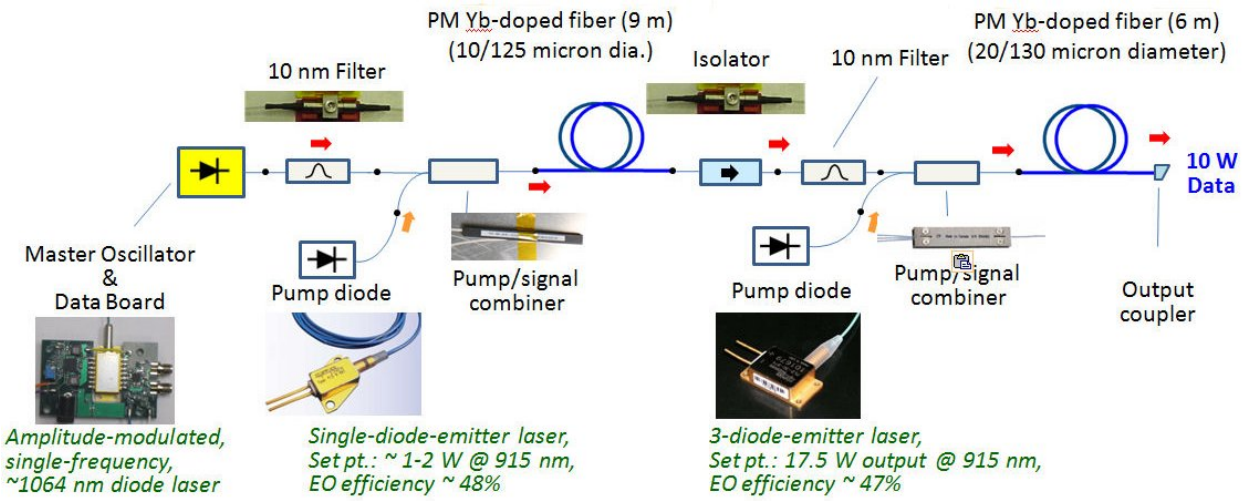

Figure 4. Schematic drawing of the laser downlink transmitter.

We switched the pump laser wavelength to 915 nm because the absorption feature at this wavelength is over 20 nm wide. Typical laser pump diodes have a temperature coefficient of ~0.3 nm/^{o}C, so this allows more than 60 ^{o}C of temperature excursion. Figure 5 shows measured output power for the fiber laser, and the second stage laser diode case temperature, the hottest component, in laboratory tests with the laser system initially at 10 ^{o}C. The second stage pump laser electrical input power was held constant at 40 W. Figure 6 is for the laser system starting at a much warmer 45 ^{o}C. Output powers of ~12 W are maintained for laser case temperatures ranging from 10 to 55^{o}C.

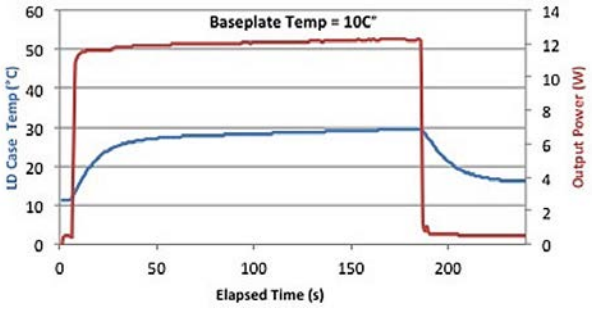

Figure 5. Second stage pump laser case temperature (blue) and fiber laser output power (red) as a function of time for a laser starting temperature of 10^{o}C.

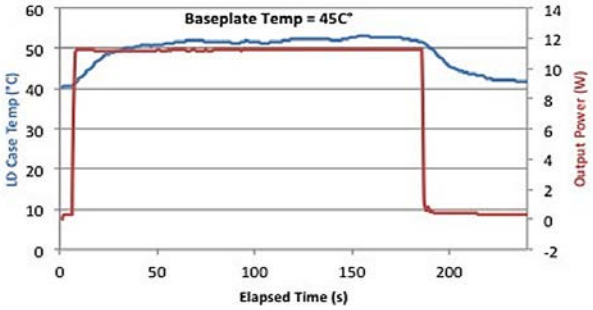

Figure 6. Second stage pump laser case temperature (blue) and fiber laser output power (red) as a function of time for a laser starting temperature of 45^{o}C.

We will operate our laser transmitter with 50 W of input electrical power and 10 W of optical output power. A 40 W heat load in a 1.5U CubeSat is a thermal challenge, and to mitigate this, we limit the "on" time of the laser transmitter to 3 minutes. This is the maximum length of time a satellite at 600-km altitude would be more than 30^{o} above the horizon for a favorable link budget. The laser system is mounted on an aluminum tray to transfer heat from the pump diodes, and this tray is thermally connected to the aluminum body. The body becomes a temporary heat sink and long-term thermal radiator. Unlike many CubeSats, our exoskeleton, or "body", is machined from a single block of aluminum to provide structural and thermal stability, and high skin electrical conductivity for passive rotational damping by Eddy currents.

The downlink laser has a FWHM beamwidth of 0.35°. This is the widest beamwidth that yields 50 Mbps data rates at half-maximum signal levels using our optical ground station located at Mt. Wilson, California. Figure 7 shows the calculated irradiance as a function of radius from the beam centerline at a range of 900 km. Also shown are expected data rates for three angles off of centerline. These rates are based on 10 W output power at the satellite, on/off modulation with an 8:1 signal-to-noise ratio, 32% atmospheric absorption and scintillation loss, and a 30-cm-diameter receive telescope with an avalanche photodiode detector with a noise equivalent power of 5 x 10^{-14} W/Hz$^{1/2}$. The intent is to receive data from the satellite at 5 to 50 Mbps rates with a bit error ratio (BER) of 10^{-4}; one bit error, on average, for every 10,000 bits received. Note that our spacecraft has better than 0.1° attitude knowledge using either the star trackers or uplink laser beacon, and 0.1° control authority using our heritage 3-axis reaction wheels.

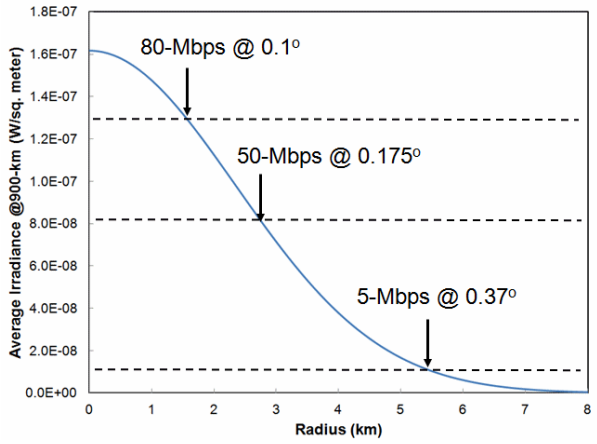

Figure 7. Average irradiance at 900-km range as a function of radius from the beam centerline for a 0.35° FHWM beam width.

6.0 THE OPTICAL GROUND STATION

We will use our Mobile Communications and Atmospheric Measurements (MOCAM) station located at Mt. Wilson, CA, as our primary optical ground station. This facility is within 50-km of our El Segundo campus and was used for tracking NFIRE. Figure 8 shows a photograph of a Meade 30-cm-diameter telescope within the telescope dome on top of a modified shipping container at Mt. Wilson. Figure 9 shows a schematic drawing of the relevant MOCAM ground station elements.

Figure 8. Photograph of our 30-cm diameter Meade receive telescope within the dome of our MOCAM optical ground station.

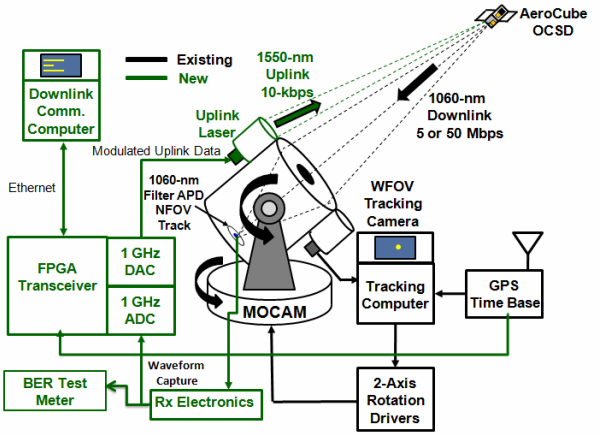

Figure 9. Schematic drawing of the MOCAM systems used in our optical ground station. New systems for this program are in green.

Rough satellite tracking will use high-accuracy ephemerides generated from spacecraft GPS fixes on previous orbits, and a wide field of view (WFOV) tracking camera will provide closed loop feedback to keep the downlink laser photons centered on the APD. This system has been used to track other LEO spacecraft and is fully capable of receiving our optical downlink. The easiest test mode is to download known data patterns and read the BER from the test meter. As we gain experience, we will download spacecraft imagery and videos, and use the FPGA transceiver to process these data.

The uplink laser provides the opportunity for closed-loop tracking of the ground station at the satellite. The 10-W, 1550-nm uplink laser is eye safe within 50 meters of the telescope, and meets FAA requirements

for operation without an aircraft spotter. We will test this laser uplink mode first, followed by the mechanically-simpler open-loop tracking mode based on star-tracker data. Long term, this could reduce ground station complexity and cost.

7.0 PROXIMITY OPERATIONS

A secondary goal of the OCSD program is to demonstrate proximity operations, and the tertiary goal is to demonstrate on-orbit propulsion. In the spring of 2015, two 1.5-U AeroCube-OCSD CubeSats will be ejected from the same P-POD. After a month of on-orbit checkout, both spacecraft will be brought within 2 kilometers of each other using variable drag for cooperative orbit rephasing, and cold gas thrusters for cross-track maneuvering. Each satellite has deployed wings that allow varying the ballistic coefficient by up to a factor of 5 by changing spacecraft orientation.

With the +Z or –Z spacecraft directions pointing in the flight direction, projected spacecraft area is about 100 cm^2. With the wings perpendicular to the flight direction, projected spacecraft area is maximized at about 500 cm^2. Unfortunately, drag in the low-drag configuration is very sensitive to pointing errors; a 10^o pitch offset increases the projected area to 185 cm^2. Our medium-drag mode has the wings parallel to the flight direction and the +Z axis zenith pointing. Projected spacecraft area in this orientation is about 150 cm^2. This mode is insensitive to small angle error about all three axes. In addition, it ensures that at least one star tracker will see stars. These high- and medium-drag modes provide a repeatable drag ratio of 3.3 to 1.

Figure 10 shows the calculated time, in days, for the chase spacecraft to match the target spacecraft altitude using 4:1 variable drag with our spacecraft, as a function of target spacecraft altitude. Naturally, the chase spacecraft has to be higher than the target. These calculations are for nearly circular orbits and include in-track corrections of up to several hundred kilometers. Our expected orbit is elliptical with a ~400-km perigee and a ~700-km apogee, and in this case, doubling the 400-km-altitude values provides a good estimate of maneuver time. Rendezvous maneuver times in excess of a month are excessive for a total 6-month on-orbit operation, and propulsion may be required to expedite the maneuver. In LEO, a 1 m/s delta-V enables an orbit altitude change of about 2 km, and we've budgeted an additional 2 m/s delta-V to handle cross-track errors that are significantly harder to correct using just differential drag.

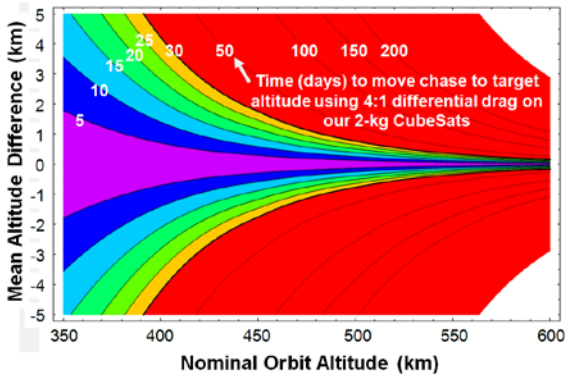

Figure 10. Time, in days, for the chase spacecraft to match the target spacecraft altitude as a function of target altitude.

Figure 11 shows the overall proximity operations concept. Differential drag and a small amount of propulsion are used to bring the chase spacecraft 2 km ahead, or behind, the target spacecraft. This staging point allows further testing of the propulsion system, initial testing of the laser rangefinder, and gaining experience with setting up Hill's orbits about a virtual spacecraft. When viewed in the co-rotating frame of the staging point, we will exercise our ability to place the chase in a co-orbit about the staging point with different mean radii and eccentricities. After this stage, we will move the chase to a starting point 1 km from the target spacecraft in a 200-meter-radius Hill's orbit about this point. A 1-cm/s in-track impulse will then put the chase in a helical trajectory that corkscrews about the target orbit and slowly translates towards, and later beyond, the target. Another 1-cm/s impulse in the opposite direction, 1 km past the target, halts the translational motion. This sequence can be reversed and repeated over 300 times without using up all of our propellant.

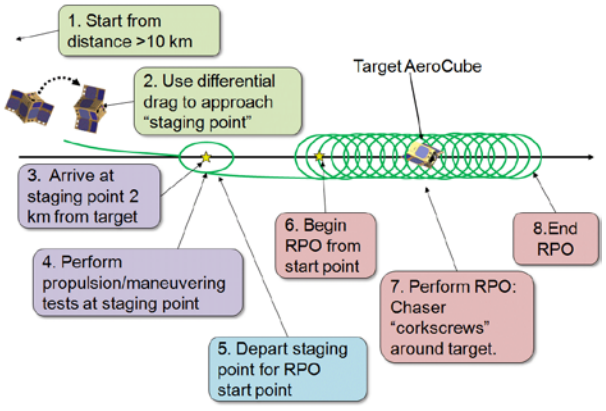

Figure 11. Maneuver sequence for our proximity operations.

Our Relative Proximity Operations (RPO) enable us to approach a 200 meter minimum range while minimizing the possibility of collision. A one-way corkscrew trajectory takes 22 hours, thus allowing us to monitor progress and abort if necessary. We plan on having four geographically-separated RF ground stations (Florida, Texas, California, and Hawaii) to provide eight or more satellite contact opportunities during an RPO. Having high-accuracy orbital ephemerides significantly reduces the possibility of collision for our trajectory. Figure 12 shows calculated chase spacecraft 3-sigma position uncertainties for radial, in-track, and cross-track errors for the week-long setup phase and RPO stage. Fortunately, multiple RPOs can be accomplished in sequence without returning to the setup phase. Note that the errors are sequentially reduced as more GPS data are incorporated and we get improved estimates of the actual spacecraft drag. This requires flying in a fixed drag orientation over eight or more days.

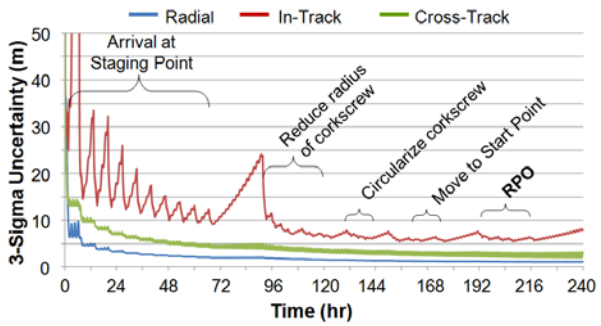

Figure 12. Chase spacecraft position errors over time as we set up and perform a relative proximity operation.

7.1 Laser Rangefinder

Section 4.2 outlined the process for aiming each +X spacecraft surface at the other spacecraft with an error of less than 0.02^{o}. Once aligned, either spacecraft can use an on-board Jenoptik DLEM-SR laser rangefinder to measure inter-satellite range to 1 meter accuracy. The GPS-based measurements are good to 10-meter error for each spacecraft, so optical ranging improves range accuracy by an order of magnitude. These range data will be used by the high-precision orbit ephemeris fitting program to further refine orbit accuracy.

Figure 13 shows a photograph of the DLEM-SR rangefinder while Fig. 2 shows its location on each spacecraft. This unit has dimensions of 5.4 cm x 2.2 cm x 3.4 cm and consumes less than 2 W during operation. It uses a 1550-nm pulsed laser with a 1.6 x 1.8 milliradian (0.09^{o} x 0.10^{o}) beam width to provide range out to 5 kilometers.[10] To get a valid return from a small CubeSat target at ranges in excess of 600 meters, we had to add a 7.1-mm diameter (~1/4") corner cube retro reflector to the +X face. The DLEM-SR provided stable (within +/- 0.2 meters) and accurate ranges over a 2.24-km-long open-air path between hilltops using this retro reflector. We added a retro reflector to each spacecraft body surface to enable ranging from optical ground stations to provide "proof" data for comparison with our high-accuracy orbital ephemerides.

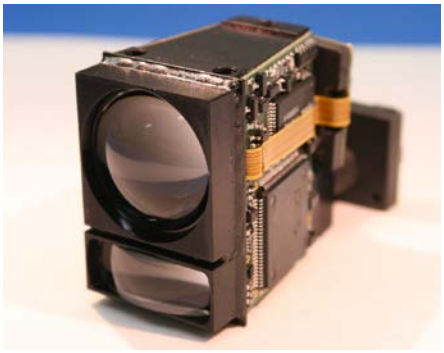

Figure 13. Photograph of the DLEM-SR Laser rangefinder.

8.0 WATER THRUSTER

We need ~3 m/s of delta-V to bring tour two CubeSats to within 1 km of each other and perform 30 sets of proximity operations. We over-sized the propulsion system to 10 m/s to account for inevitable mis-steps in orbit control and to allow for multiple tests of collision avoidance maneuvers. If all CubeSats had the ability to maneuver away from a potential collision with another space object, there would less concern in the overall Space Community about the rapidly increasing numbers of CubeSats on orbit.

Our chief concern was to design and build a propulsion system that had low mass, low power requirements, and a minimum number of ground tests and documentation required for integration into a P-POD. We've flown cold gas and solid rocket thrusters on spacecraft ejected by the U.S. Space Shuttle, and wanted to minimize the costs associated with propulsion system integration and safety requirements.[11,5]

The easiest propulsion systems to flight qualify are those with low thrust (this prevents significant changes in orbital elements that can confuse ground-based tracking systems), have minimum explosion hazard during launch, and use non-toxic, non-reactive propellants. We ended up borrowing a propulsion system from the ancient Greeks; Hero's steam thruster. Water has a low molecular weight, thus offering a roughly 100-s specific impulse at room temperature, a

vapor pressure significantly below 1 atmosphere at room temperature to eliminate the use of pressure vessels, is relatively inert with respect to most launch vehicle components, and is non-toxic in the quantities required (about one ounce, or a full shot glass). A 1st century, or even 18th century "steam punk," thruster actually makes sense for 21st century CubeSats.

A water thruster has flown on the University of Surrey Space Center STRaND-1 CubeSat; the Water-Alcohol Resistojet Propulsion, or WARP drive.[12] We decided to forgo the alcohol in order to minimize flammability hazards on the launch vehicle, not to mention our laboratory. Alcohol or other compounds are typically added to water to lower the freezing point and prevent tank and tubing rupture. Our approach is to use a propellant management system that holds the water, or ice, within an expandable volume that cannot touch the propellant tank walls. Freezing of water does not compromise the propulsion system structure.

A key challenge in designing a water thruster system for a CubeSat is to provide the required level of thrust at low vapor pressure. Figure 14 shows the vapor pressure of water as a function of temperature. We intend to operate the thruster with a propellant temperature of 40 °C. This generates a vapor pressure of 6.9 kPa (1 psi), and a thrust level of 0.36 mN using a nozzle throat diameter of 700 microns. Figure 15 shows measured thrust as a function of tank pressure. We carefully chose the valves to provide the required flow rate to generate 3 to 5 mN of thrust. Our flow system uses two parallel strings of two series-connected valves to provide increased thruster system reliability. It is tolerant to an open or closed failure of any individual valve.

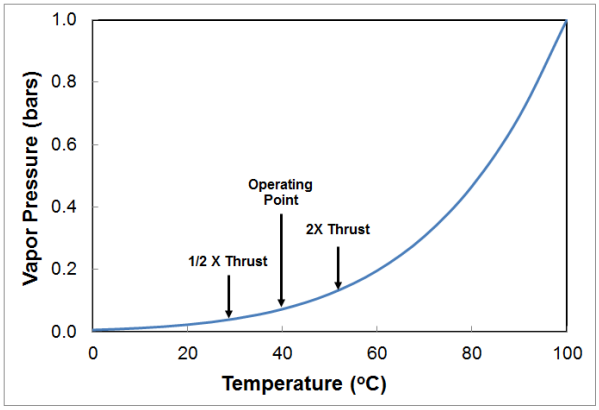

Figure 14. Vapor pressure of water as a function of temperature. Pressure at 40 °C is 6.9 kPa.

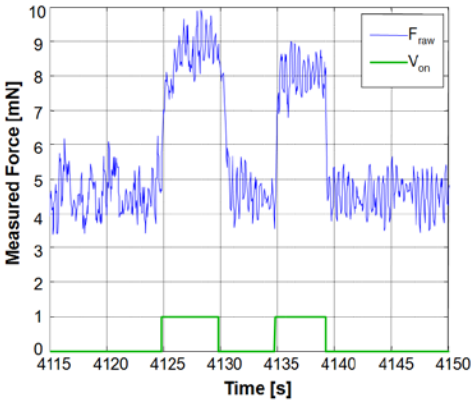

Figure 15. Measured thrust as a function of tank pressure using water as a propellant.

This propulsion system, like the one we flew on MEPSI in 2006,[11] is fabricated out of plastic using additive manufacturing. The propellant tank and feed lines are voids in a single block of plastic. MEPSI had a plastic converging/diverging nozzle integrated into the structure, but for this project, we used an aluminum nozzle with a 700-micron-diameter machined throat. Figure 16 shows a photograph of an early prototype for thrust testing. The nozzle mounts in the protrusion near the bottom center, and the valves have been upgraded in number (to allow parallel paths for improved reliability) and in flow capacity.

Figure 16 Photograph of a prototype thruster for initial thrust testing.

9.0 SUMMARY

The NASA OCSD effort is a subsystem flight validation mission to test commercial-off-the-shelf components and subsystems that will enable new communications and proximity operations capabilities for CubeSats and other spacecraft. It will demonstrate optical communications using milliradian beam spreads

that are compatible with near-term CubeSat pointing capabilities. The baseline mission will use a ~10-W modulated fiber laser with a 0.35° angular beamwidth on a 1.5U CubeSat (AeroCube-OCSD) and a 30-cm-diameter telescope located on Mt. Wilson in southern California to receive optical pulses. We plan on demonstrating 5-Mbps and 50-Mbps optical downlinks. In addition, the spacecraft will also flight test a laser rangefinder system, aerodynamic drag control, a miniature pair of star-trackers, and a steam thruster.

In early 2015, two 1.5U AeroCube-OCSD CubeSats will be ejected from the same P-POD and brought within 2 km of each other using on-board GPS for position and velocity determination, variable drag for cooperative orbit rephasing, and cold gas thrusters for cross-track maneuvering. We plan on bringing the two spacecraft within 200 meters of each other using a helical trajectory that minimizes the risk of accidental contact.

References

1. H. Smith, S. Hu, and J. Cockrell, "NASA's EDSN Aims to Overcome the Operational Challenges of CubeSat Constellations and Demonstrate an Economical Swarm of 8 CubeSats Useful for Space Science Investigations," paper SSC-XI-2, AIAA/USU Small Satellite Conference, Logan, Utah, August 10-15, 2013.

2. Fields, R., Kozlowski, D., Yura, H., Wong, R., Wicker, J., Lunde, C., Gregory, M., Wandernoth, B., and Heine, F., "5.625 Gbps Bidirectional Laser Communications Measurements Between the NFIRE Satellite and an Optical Ground Station," Proc. of the 2011 Int. Conf. on Space Optical Systems and Applications, pp.44-53, Santa Monica, CA, 11-13 May, 2011.

3. Heine, F., Kampfner, H., Lange, R., Czichy, R., Meyer, R., and Lutzer, M., "Optical Inter-Satellite Communication Operational," 2010 Military Communications Conference, pp.1583-1587, San Jose, CA, Oct. 31 – Nov. 3, 2010.

4. Janson, S.W., and Welle, R.P., "The NASA Optical Communication and Sensor Demonstration Program," paper SSC13-II-1, AIAA/USU Small Satellite Conference, Logan, Utah, August 10-15, 2013.

5. Siegfried W. Janson, Brian S. Hardy, Andrew Y. Chin, Daniel L. Rumsey, Daniel A. Ehrlich, and David A. Hinkley," Attitude Control on the PicoSatellite Solar Cell Testbed-2," paper SSC12-II-1, 26th Annual AIAA/USU Conference on Small Satellites, Logan, Utah, August, 2011.

6. Siegfried W. Janson and David J. Barnhart, "The Next Little Thing: Femtosatellites," paper SSC13-VI-3, 27th Annual AIAA/USU Conference on Small Satellites, Logan, Utah, August, 2013.

7. Melexis Microelectronic Systems, MLX90620 datasheet, URL: http://www.melexis.com/Assets/Datasheet-IR-thermometer-16X4-sensor-array-MLX90620-6099.aspx, Melexis Microelectronic Systems, Ieper, Belgium, May 2013.

8. Sensonor AS, Butterfly Gyro STIM210 Multi-Axis Gyro Module datasheet, URL: http://www.sensonor.com/media/90317/datasheet%20stim210%20ts1545.r10.pdf, Sensonor AS, Horton, Norway, May 2013.

9. VectorNav Technologies, VN-100 web page, URL: http://www.vectornav.com/products/vn100-smt , VectorNav Technologies, Dallas, TX, 2014.

10. Jenoptik, DLEM-SR Datasheet, Jenoptik Defense and Civil Systems, Jena, Germany, URL: http://www.jenoptik.com/cms/products.nsf/0/645924FE73AE3A1EC125790A0037F7ED/$File/dlem_sr_en_web.pdf?Open , June 2014.

11. Hinkley, D., "A Novel Cold Gas Propulsion System for Nanosatellites and Picosatellites, paper SSC08-VII-7, 22nd Annual AIAA/USU Conference on Small Satellites, Logan, Utah, August 2008.

12. Surrey Satellite Technology, Ltd., "Space Blog, Warp Speed Ahead!," URL: http://www.sstl.co.uk/Blog/January-2013/WARP-speed-ahead , Surrey Satellite Technology, Ltd., Guidford, Surrey, the United Kingdom, June 2014.